ISSN 2314-5609
Nuclear Sciences Scientific Journal
vol. 3, p 107 - 122
2014

Nuclear Materials Authority
P.O.Box 530 Maadi, Cairo, Egypt

GEOCHEMICAL AND MINERALOGICAL CHARACTERIZATION OF NATASH VOLCANICS, SOUTH EASTERN DESERT, EGYPT\

MOSTAFA E. DARWISH and AMIRA M. EL-TOHAMY
Nuclear Materials Authority

ABSTRACT

The two ring structures of Western Ghurfa and Gaziret Khashm Natash as well as the ring dyke, G. El Ghurfa have extruded through the volcanic flows. The three rings range in composition from volcanic flows, represented by trachybasalt, trachyandesite, normal trachyte and alkaline trachyte and pyroclastic rocks (agglomerates, tuffs, pumice and scoria). The rings are semicircular to circular in outline range from 1 km to 0.6 km.

The high contents of uranium in the studied rocks are due to the presence of secondary uranium minerals such as meta-autunite and kasolite as well as the accessory minerals bearing uranium such as monazite, xenotime, zircon and allanite.

The geochemical studies of the volcanic rocks revealed that the rock samples fall in the trachyte, trachyandesite , trachybasalt and basalt fields. These rocks were originated from alkaline magma, and developed in continental basalt environment. The enrichment of the LREEs (182 - 391 ppm) is most due to the presences of garnet in the source.

INTRODUCTION

Wadi Natash volcanics is a part of phanerozoic volcanic activity in the south Eastern Desert of Egypt. They cover an area about 130 km^2, lie about 125 km east north east of Aswan along the boundary between the Nubian sandstones and the Precambrian rocks (Fig.1).

Wadi Natash volcanics form dissected plateau with stratified appearance which trends approximately NNW-SSE. This plateau is formed of thick piles of volcanic flows; each of them does not extend laterally more than 6 km. In places these piles appear as relics of adjacent former volcanoes with their lava field superimposed on one another. The east and northeast of the area are occupied by the lava flows, a great number of volcanic necks and plugs occur in a dispersed fashion. Wadi Natash volcanics and their volcaniclastic sediments are extending nearly parallel to the boundary between the (upper and lower) Nubian sandstones.

The geology of Wadi Natash were studied by many authors e.g. Barthoux (1922) ,El Ramly et al.(1971), Abul Gadayel (1974), Hubbard (1981) ,Coulter (1981), Hashad et al. (1982), Crawford (1984) and Mohamed (2001). Whereas Natash volcanics age (104±7 Ma) were determined by Hashad and El Reedy (1979), Abul Gadayel, (1974) and Ressetar et al. (1981) using Rb/Sr isochron and K/Ar methods. Recently the present work aims to study in detail the geochemical characteristics of Natash volcanics south Eastern Desert, Egypt, as well as mineralogical and radioactivity studies to elucidate the petrogenesis of the three rings on the study area.

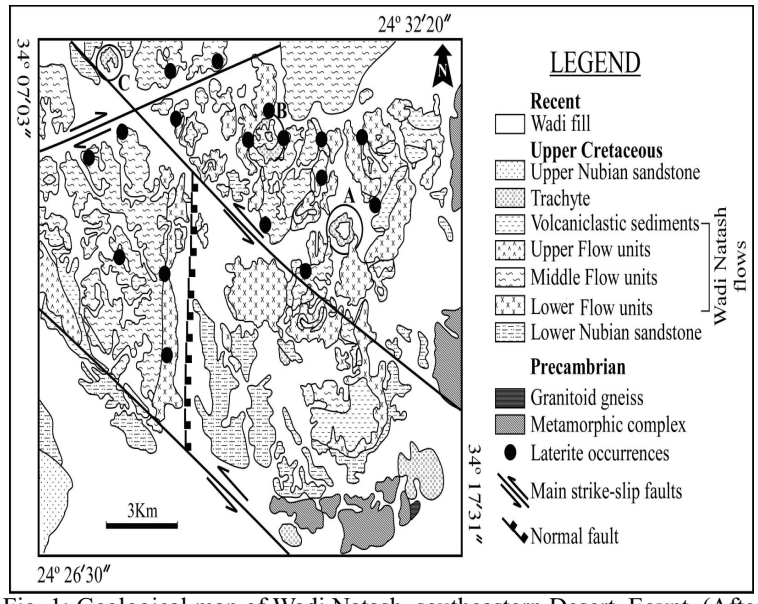

Fig. 1: Geological map of Wadi Natash, southeastern Desert, Egypt. (After Crawford, 1984 and modified by Ibrahim, 2010)

GEOLOGICAL SETTING

Wadi Natash volcanic rocks can be arranged based on field geology and structure observations beginning with the oldest (Fig.1): a)-metasediments (amphibolite schist, and mica schist), b)-lower Nubian sandstones (quartz arenite, greywacke, and calcareous sandstone), c)-volcanic flows (basalt, trachybasalt, trachyandesite, trachyte and pyroclastics) and d)-finally the Upper Nubian sandstone outside the mapped area (Ibrahim, 2010).

The volcanic sequence is represented by three distinct flow units, separated by two sequences of pyroclastics (volcaniclastic sediments). Each of the three flow units shows a gradual change in composition upwards from alkali olivine basalt through trachybasalts, trachyandesites, to trachytes. The thickness of the volcanic flow decreases at the westernside of Wadi Natash (50 m) and increases at their eastern part (250 m). The volcanic sequences and their intercalated volcaniclastic sediments dip 50 to westwards (Ibrahim, 2010). The regional westward dip is the result of displacement along NW-SE and NE-SW strike- slip faults with left- hand and right-hand movement's respectively. The pyroclastics comprise agglomerates and tuffs (Figs.2-5). Also N-S normal faults with obvious displacements are common, and show different degrees of fault cataclases and breccias. Pumice rock which is characterized by vugs occupied by carbonates (Fig.6) and scoria rock which is characterized by basaltic composition are recorded in Wadi Natash.

Fig.2: Photograph showing Trachyte plug, Wadi Natash area

Fig.3: Photographs showing Maroon and white tuffs, Wadi Natash

Fig. 4: Photographs showing Layered tuffs, Wadi Natash, looking SE

Fig. 5: Photographs showing Pebbles and cobbles in agglomerate, Gaziret Khashm Natash, looking SW

Fig.6: Photographs showing pumice, Wadi Natash area

Many volcanic domes, necks and trachyte plugs occur in a dispersed fashion in the Eastern sector have extruded through the three flow units. Three of these plugs were found as rings; namely G. El Ghurfa, Gaziret Khashm Natash and Western Ghurfa.

Gabal El Ghurfa

It consists mainly of normal trachyte and alkaline trachyte at the outer zone which characterized by high relief and columnar joints (Fig.7) and forms a ring dyke with a diameter of 1 km (Fig. 8). The inner zone (600 m in diameter) of the ring dyke is mainly represented by Lower Nubian sandstones (LNSS) a small trachyte plug with unconformity surface between them. The LNSS are composed of quartz arenite, greywacke and calcareous sandstone at the base followed by conglomerate at the top (Ibrahim et al., 2013).

Fig.7: Photographs showing Columnar joints in trachyte, G. El Ghurfa, southeastern Desert, Egypt

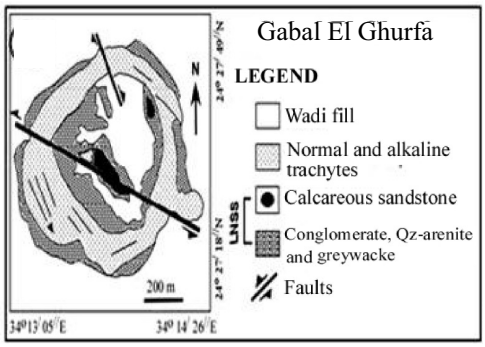

Fig.8: Geological map of G.El Ghurfa ring dyke, Wadi Natash Southeastern Desert, Egypt

Gaziret Khashm Natash

Gaziret Khashm Natash lies at the mouth of Wadi Natash and forms a horse shoe-ring structure ~0.6 km in diameter (Fig.9). It is represented by volcanic flow (trachybasalts and trachyandesites) and pyroclastics (tuffs and agglomerates).

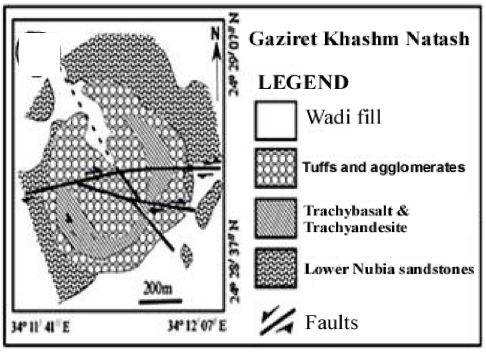

Fig.9: Geological map of Gaziret Khashm Natash, Wadi Natash Southeastern Desert, Egypt

It was extruded in the Lower Nubian sandstone at their outer parts. Agglomerates occur in the inner zone as two layers composed of pebbles and cobbles of flow debris in coarse to fine grained matrix of lithic fragments (mainly basaltic , andesitic and trachytic in composition). The pebbles and cobbles are semi-rounded, range in size from few cm to 40 cm in diameter and its color ranges from black, grey to yellow. The tuffs are exposed at the highest topographic levels, and composed of crystal tuffs (feldspars, quartz, and mafics) embedded in fine-grained cryptocrystalline groundmass. Gaziret Khashm Natash dissected by two sets of faults. The first one is the oldest and running NW-SE with (left lateral movement) and displaced by the second one which running nearly WNW-ESE with (right lateral movement).

The Western Ghurfa

It constitutes an incomplete ring structure ~0.7 km in diameter and consists mainly of lower(Fig.10), middle and upper flows (trachybasalts, trachyandesites, normal and alkaline trachytes) as well as agglomerates and tuffs with gradational contacts due to differentiation. The volcanic flows were extruded in the Lower Nubian sandstone. The ring has been dissected by a series of WNW-SSE oldest faults which dissected by the youngest NNE-SSW parallel faults with right lateral movements.

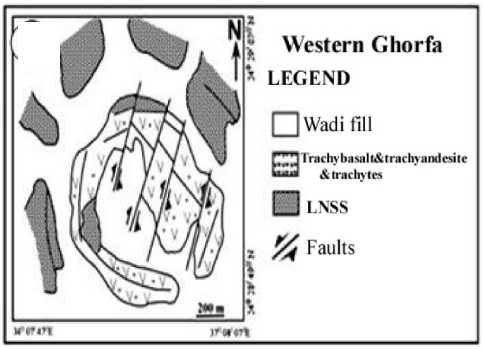

Fig.10: Geological map of western Ghurfa, Wadi Natash Southeastern Desert, Egypt

METHODOLOGY

The major oxides were analyzed using conventional wet chemical techniques of Shapiro and Brannock (1962). The X-ray fluorescence technique (XRF) was used to determine the trace element contents using PHILIPS X'Unique-II spectrometer as well as rare trace elements carried out at ACME analytical LTD, Vancouver, Canada.

The XRD technique (PHILIPS PW 3710/ 31 diffractometer) and environmental scan-

ning electron microscope (ESEM) was used to identify the unknown minerals. The EDAX analysis is considered as semi-quantitative analysis since oxygen, carbon and hydrogen are not analyzed. For the radiometric study, a multichannel analyzer Gamma ray spectrometer was used to determine the eU and eTh concentrations in the laboratory. All of the previously mentioned analyses were measured in the laboratories of the Nuclear Materials Authority of Egypt.

MINERALOGY AND RADIOACTIVITY

Meta-autunite [Ca $(UO_2)2(PO_4)2•3(H_2O)$] and kasolite [Pb (UO_2) $SiO_4.H_2O$] are secondary minerals common in Gaziret Khashm Natash and Western Ghurfa. The presence of secondary uranium minerals in the trachyte rocks is due to the uranium-bearing hydrothermal solutions which associated with these rocks and filling the vugs and fracture planes in trachyte of G. El Ghurfa, trachyandesite in both of Gaziret Khashm Natash and Western Ghurfa.

Meta-autunite[Ca $(UO_2)2(PO_4)2•3(H_2O)$]

It is a dehydration product of autunite (Fig.11). Meta-autunite is ranges in color from lemon-yellow, greenish yellow to canary yellow.

Kasolite [Pb (UO_2) $SiO_4.H_2O$]

It is detected as separate mineral in trachyte of Gabal El Ghurfa and trachyandesite of Gaziret Khashm Natash and Western Ghurfa as fine bright spots between feldspars(Fig.12). Microscopically, kasolite occurs as massive granular masses having resinous to greasy luster and lemon yellow color.

Molybdite (MoO_3)

It is a secondary mineral created by oxidation of molybdenite. It occurs as flat needle or thin plates on the cavities or coating molybdenite in trachybasalt of Gaziret Khashm Natash and Western Ghorfa, (Fig. 13).

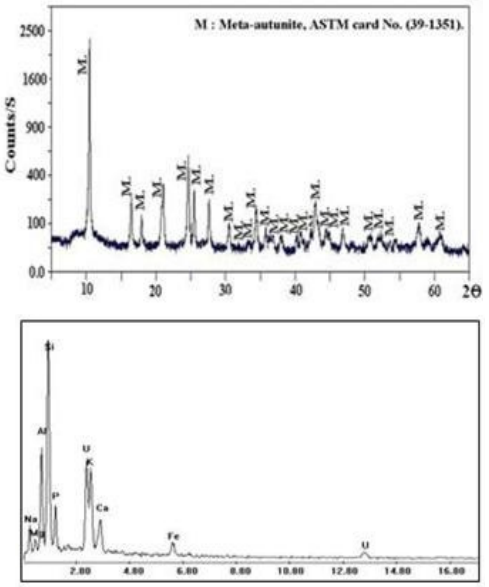

Fig.11: X-ray diffractogram and EDX spectrum of meta-autunite

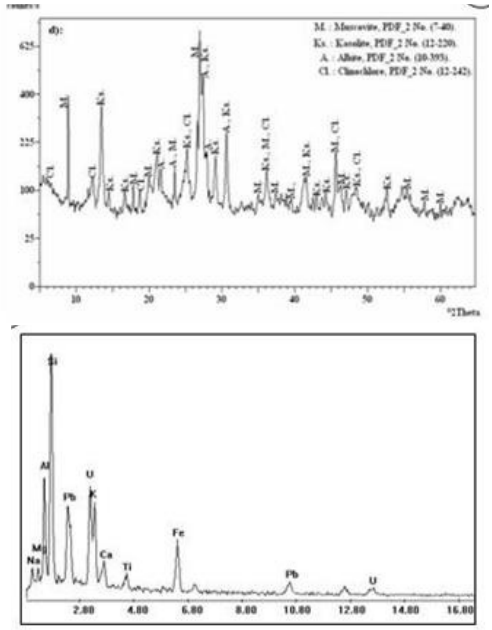

Fig.12: X-ray diffractogram and EDX spectrum of kasolite, which recorded at G. El Ghurfa, Gaziret Khashm Natash and Western Ghurfa, south Eastern Desert.

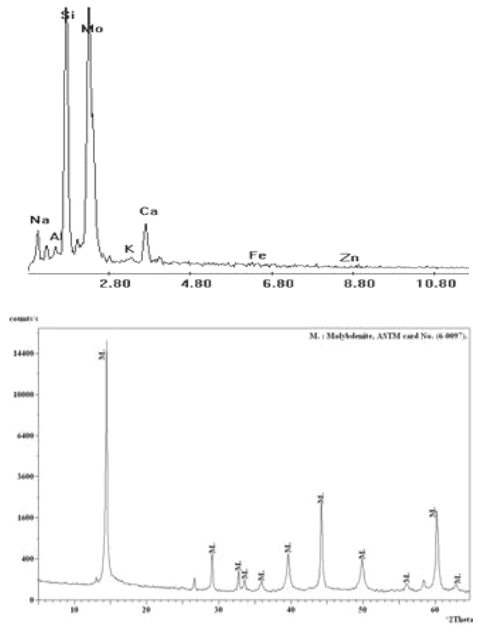

Fig.13: X-ray diffractogram and EDX spectrum of molybdite mineral

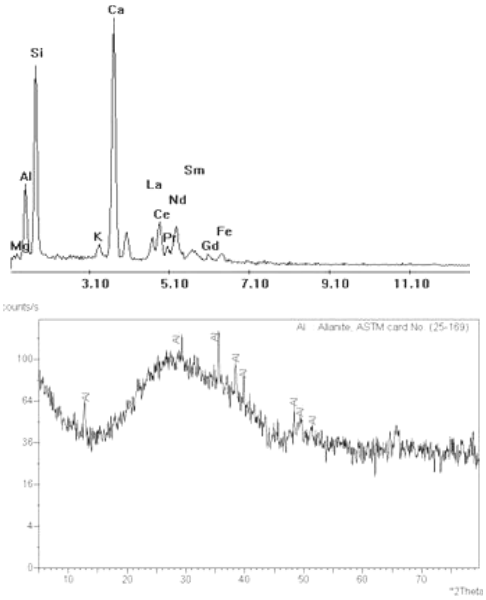

Fig.14: X-ray diffractogram and EDX spectrum of allanite minerals which recorded at G. El Ghurfa, Gaziret Khashm Natash and Western Ghurfa, south Eastern Desert

Allanite [(Ca, Ce, La, Y) 2(Al, Fe)$_3$(SiO$_4$)$_3$(OH)]

It is a uranium and thorium carrier and altered to an amorphous substance product by break down of the space lattice by radioactive emanation (Kerr, 1977). It is found as inclusions in trachyandesite of Gaziret Khashm Natash and Western Ghurfa. (Fig. 14).

Monazite [(Ce, La, Th, Nd, Y) PO$_4$]

It is an important ore for thorium, lanthanum, and cerium. Monazite was recorded in trachyte of Gabal El Ghurfa and trachyandesite of Gaziret Khashm Natash aswell as Western Ghurfa, (Fig.15).

Xenotime (YPO$_4$)

It is recorded in trachyte of G. El Ghurfa, as small bright spots on the surface on the rock. The X-ray diffraction analysis and EDX detected the presence of xenotime (Fig. 16).

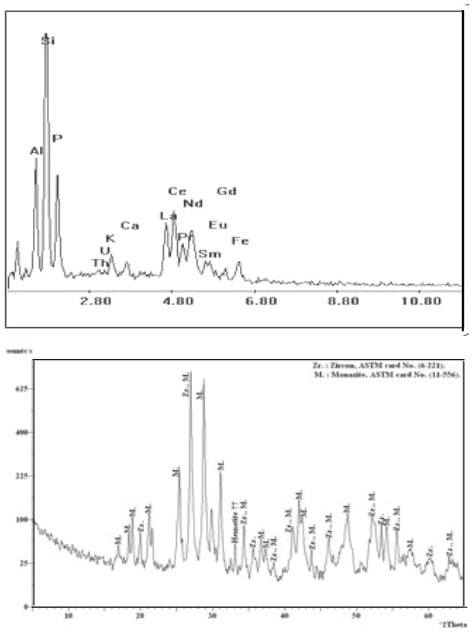

Fig.15: X-ray diffractogram and EDX spectrum of monazite mineral

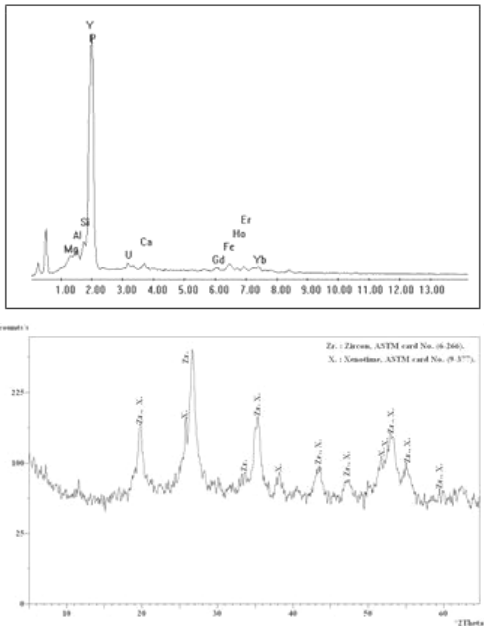

Fig.16: X-ray diffractogram and EDX spectrum of xenotime minerals which recorded at G. El Ghurfa, Gaziret Khashm Natash and Western Ghurfa, south Eastern Desert.

CHEMICALLY URANIUM DETERMINED VS. RADIOMETRIC URANIUM

Thirty samples representing trachyte, trachyandesite, tuffs and agglomerates which exposed in Natash volcanics are analyzed for their equivalent uranium and equivalent thorium contents. Table (1) shows the range of the radiometric measurements in the Natash volcanics and eTh/eU as well as eU/eTh ratios.

The low average Th/eU ratio (0.29) and the high eU/eTh ratio (4) in the studied G. El Ghurfa trachyte samples is due to the effect of Na- and K- metasomatism which causes significant enrichment of uranium (20-51) and consequently a marked disequilibrium (Fig.17). The high eU/eTh ratio in G. El Ghurfa indicates that the radioelement distribution is governed by post magmatic redistribution in Wadi Natash and this could be a favorable economic criterion into zones within the volcanic rocks. The studied trachyte plug of G. El Ghurfa possess radioactive anomalies of uranium mineralization as a result of investigating them with hydrothermal solution through fissures and cracks.

Hansink (1976) and Stuckless et al. (1984) defined the D-factor which represented the ratio between the chemically determined uranium and the radiometrically measured uranium. They considered that if the D-factor is more or less than unity, it indicates addition or removal of uranium respectively. It is clear that the chemically determined uranium contents of all samples is greater than the measured radiometric uranium (range from 5.5-14) i.e. addition of uranium (Table .1). The presence of channel ways in the G. El Ghurfa trachytic ring dyke (WNW-ESE and NNW-SSE,) give the structural control favorable for the migration of the uranium-rich residual fluid which probably formed uranium mineralization in both the LNSS and trachytic rocks of G. El Ghurfa ring dyke.

Table 1 : Ranges and averages of radio-elements distribution in the Natash volcanic rocks

Rock type	Radio-elements					
	eU (ppm)	eTh (ppm)	eTh/eU	eU/eTh	U_{ch} (ppm)	D. factor U_{ch}/eU
Trachyte	35	10	0.29	4	197	5.5
N=10	(20-51)	(5-16)	(0.11-0.43)	(2.3-9)	57-290	
Trachyandesite	10	5	0.3	2	190	19
N=10	(3-15)	(2-7)	(0.11-0.63)	(1.6-3)	(85-275)	
Tuffs and Agglomerates	14	4	0.25	3	201	14
N=10	(6-21)	(1-5)	(0..1-0.4)	(2.4-4)	(154-270)	

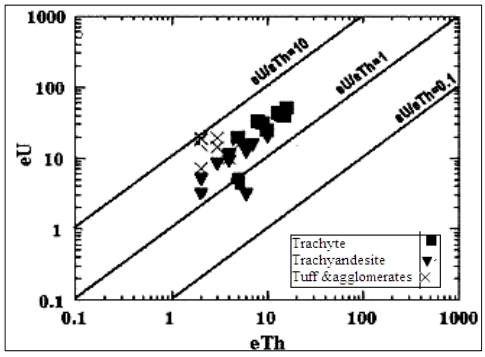

Fig. 17: eU vs. eTh for Natash volcanic rocks

The presence of supergene secondary uranium minerals (meta-autunite and kasolite) indicate that such rocks in Natash volcanics were subjected to active hydrothermal convective cells and the accessory minerals controlled the fractionation of uranium and thorium in the studied rocks.

GEOCHEMISTRY

Major oxides (wt%) and some trace elements (ppm) of thirty two representative samples from Natash volcanic rocks (10 trachyte samples, 11 trachyandesite samples, 4 trachybasalt samples, 4 basalt and 3 pumice samples) are analyzed. The analytical data are given in Table 2. Some geochemical indices and some elemental ratios are listed in Table 3 as well as eleven representative samples are analyzed for rare earth elements (in ppm) are presented in Table (4) .

Table 2 : Average and range of representative major oxides (wt%) and trace elements (ppm) contents of Natash volcanics

Rock Type	Trachyte	Trachyandesite	Trachybasalt	Basalt	Pumice
NO.	(N=10)	(N=11)	(N=4)	(N=4)	(N=3)
Average and range of major oxides (wt %)					
SiO_2	64.5 (60- 66.6)	60 (58 - 61)	50 (48.6 – 50)	31.6 (36.7 - 1.7)	45.6(45 - 46.4)
Al_2O_3	13.4 (11.3 - 5.4)	14(12.5 - 16.2)	17(16.3 - 17.4)	15.7(13.3 –18)	14 (13 - 2.30)
TiO_2	0.4 (0.04 - 1.2)	0.8(0.34 - 1.1)	1(0.41 - 1.2)	3.2(1.2 - 4.1)	3.2 (2.6 - 3.90)
FeO	5.3 (3.4 – 6)	8.8(3.7 - 12.2)	11.7(9.7 - 3.7)	12.5(6.5 - 5.8)	6.20(4.5 – 9)
Fe_2O_3	6 (3.7 - 6.6)	10(4.0 - 13.5)	13(10.8 - 15.2)	14(7.2 - 17.6)	8(7.2 - 9.3)
MnO	0.2 (0.03 - 0.4)	0.2(0.0 - 0.5)	0.4(0.0 - 0.6)	--	0.2(0.2 - 0.2)
CaO	1.8 (0.4 - 3.5)	3(1.4 - 4.7)	6.6(5.6 - 6.7)	2.8(2.8 - 2.8)	8.8(7.4 - 10.2)
MgO	1 (0.5 - 1.4)	1.2(1.0 - 1.5)	2(2 – 2)	1.1(1.0 - 1.2)	7.5(5.9 - 9.8)
Na_2O	6.6(5.4 - 7.8)	7.2(6 - 8.6)	4.8(3.5 - 6.1)	11(8.8 - 13.5)	3.1(2.9 -3.5)
K_2O	4.6(3.7 - 5.3)	2.2(0.2 - 2.7)	1.5(0.4 - 2.2)	1.0(0.6 - 1.6)	1.2(1.03-1.8)
P_2O_5	0.33(0.01 - 0.5)	0.4(0.1 - 0.7)	0.4(0.7 - 0.3)	0.6(0.4 - 0.8)	0.7(0.6 -0.8)
L.O.I	1.4(0.8 - 2.3)	2(1.1 - 2.9)	3.1(2.2 - 3.9)	4.2(1.7 - 5.6)	1.4(0.73-1.8)
Total	99.3(98.3 – 100)	99(98 - 99.6)	98.5(98.2 - 98.9)	98.5(98 - 99.2)	99.7(99.1-100.3)
Average and range of representative trace elements (ppm)					
Ba	1158 (132 – 1859)	78 (204 – 1525)	1111(721-1572)	555(315-1463)	546(514-595)
Cu	13.7 (2.3-23)	85.6 (1.99-776)	20 (3-35)	un	33 (17-43)
Pb	11(4-37)	20 (3.6-61)	11(8.5-15)	un	8.5 (2.3-12.5)
Zn	181(109-277)	439 (133-1402)	195(167-459)	un	135(101-200)
Ni	3(1-8)	11(0.4-38)	17(1-29)	134(44-348)	134(45-190)(
Zr	705(167-1485)	1085(65-3063)	316(22-670)	234(195-348)	27(24-30)
Y	39(6-100)	62 (7-179)	34(2-72)	27(25-35)	2 (2-2)
Rb	39 (8-111)	60(10-208)	42(7-86)	19(7-29)	6(3-8)
Nb	76(2-235)	161(5-4960)	77 (8-235)	52(39-560)	78(73-82)
Sr	324(49-657)	238(68-633)	270(159-352)	725(619-979)	385(378-392)
U	197(57-290)	190(85-275)	196(118-271)	1.2(0.99-1.3)	211(154-270)
Th	56 (20-95)	55(30-85)	43(25-60)	0.40(3.4 -5)	52(20-72)
Cr	9.1(5-16)	10(5-24)	9(5-27)	229(80-402)	6(5-7)
Ga	25(10-47)	28.4(17-30)	23(22-33)	u.d	17(14-21)
V	110 (1-418)	34(1-135)	111((56-147)	u.d	66(62-71)
W	1.600.8-3.2)	1.4(0.9-2.5)	u.d	u.d	u.d
Sn	7.4(4.3-13.1)	4.1(3.9-4.3)	u.d	u.d	u.d
Be	5.3(3-10)	2.3(1-3)	u.d	u.d	u.d
Sc	5.8(0.2-8.8)	9.4(9-10)	u.d	u.d	u.d
Ta	9(6-14)	5(4-6)	u.d	4(3-4)	u.d
Cs	0.6(0.2-1.3)	0.2(0.1-0.2)	u.d	u.d	u.d
Mo	6.4(3-12)	4(3-5)	u.d	u.d	u.d
Co	6(1-8)	13(7-21)	u.d	u.d	u.d
As	1.7(1.4-2)	1.73(1.6-2)	u.d	u.d	u.d
Cd	1.1(0.27-2.18)	0.35(0.27-0.6)	u.d	u.d	u.d
Sb	0.2(0.12-0.45)	0.1(0.08-0.11)	u.d	u.d	u.d
Hf	18(13-28)	12(10-14)	u.d	6(5-7)	u.d
Li	7(5-10)	8(6-11)	u.d	u.d	u.d

u.d=under limit of detection. N= number of analyzed samples

Table 3 : Some geochemical indices and elemental ratios of Natash volcanic rocks

Rock Type	Trachyte	Trachyandesite	Trachybasalt	Basalt	Pumice
No. of samples	(N=10)	(N=11)	(N=4)	(N=4)	(N=3)
Diff-index	80(76-83)	71(63-78)	48(44-52)	37(34-41)	80(76-83)
Agpaitic-index	1(1-1.5)	1(0.8-1)	0.6(0.4-0.6)	0.5(0.4-0.5)	1(1-1.5)
Alkalinity ratio	6(4-12)	4(2-7)	1.7(1.6-2)	1.5(1-2)	6(4-12)
Na_2O/K_2O	1.5(1.4-2)	7(2-20)	6(2-16)	18(18-19)	1.5(1.4-2)
Th/U	0.3(0.1-0.4)	0.3(0.2-0.4)	0.2(0.1-0.4)	0.2(0.1-0.3)	0.3(0.1-0.4)
Ba/Y	52(26-135)	34(1-46)	121(9-360)	277(257-297)	52(26-135)
Ba/Sr	5(1.5-7)	4.6(0.6-9)	4(3-6)	1.5(2-2.5)	5(1.5-7)
Sr/Y	12(0.5-29)	8(0.3-20)	50(2-176)	192(189-196)	12(0.5-29)
Zr/Y	22(13-41)	17(9-26)	14(2-22)	14(12-15)	22(13-41)
Zr/Rb	21(15-50)	49(2-346)	9(2-15)	6(4-8)	21(15-50)
Nb/Y	1.5(0.2-5)	4(0.2-22)	8(0.3-29)	38(36-41)	1.5(0.2-5)
Nb/U	0.6(0.01-4)	0.6(0.02-2)	0.2(0.03-0.4)	0.4(0.3-0.4)	0.6(0.01-4)
Rb/Sr	0.4(0.03-2)	0.5(0.01-3)	0.2(0.02-0.5)	0.01(0.01-0.02)	0.4(0.03-2)
Th/Nb	7.5(0.1-30)	4(0.2-15)	4(1-8)	0.6(0.2-0.8)	7.5(0.1-30)
Ba/Nb	150(0.5-407)	46(2-305)	97(3-196)	7(7-7.2)	150(0.5-407)
Ba/Zr	2.4(0.1-5)	2.2(0.07-12)	11(3-33)	20(20.3-21)	2.4(0.1-5)
Na_2O/K_2O	1.5(1.4-2)	7(2-20)	6(2-16)	18(18-19)	1.5(1.4-2)

N= number of analyzed samples

Table 4: The rare earth elements (ppm) of the studied volcanic rocks

					Rock types		
REE (ppm)	Trachyte N=4	Trachyandesite N=3	Basalt N=4	elemental parameters	Trachyte N=4	Trachyandesite N=3	Basalt N=4
La	39.3	58	84	∑REEs	203	311	435
Ce	81	133	185	∑LREEs	182	281	391
Pr	10	15.57	22	∑HREEs	21.8	30	44
Nd	41	61.5	83	LREEs/HREEs	8.35	9.50	9
Sm	8.4	10.5	14	La/Yb	17.4	22.4	20
Eu	3	3	3	La/Sm	5	58	84
Gd	8	9.10	12	Gd/Lu	22.95	133	185
Tb	1.10	1.43	2	Gd/Yb	3.53	15.57	22
Dy	6	8.4	13	Tb/Yb	0.5	0.4	0.3
Ho	1	2	3	Ce/Yb	35.7	35.7	30.8
Er	2.8	4.23	7	Eu/Sm	0.32	0.29	0.21
Tm	0.5	0.53	1	Eu/Eu*	0.9	0.9	0.7
Yb	2.3	4	6				
Lu	0.35	0.57	1				

General Geochemical Features

1- The average of the calculated differentiation index (DI= Qz + Or + Ab) of Thornton and Tuttle (1960) are 80%, 71%, 48%, 37% and 60% of the rock composition for trachyte, trachyandesite, trachybasalt, basalt and pumice volcanic rocks respectively.

2- The agpaitic index was expressed as the molecular ratio of Na_2+K_2O / Al_2O_3.If the index is higher than 1, the rock is agpaitic and is usually characterized by high contents of Na, Fe, Cl, and Zr with low Mg and Ca. The index average is 1, 1, 0.6, 0.5 and 1 of the rock composition for trachyte, trachyandesite, trachybasalt, basalt and pumice volcanic rocks respectively.

3- The alkalinity ratio is being on 12.15, 3.9, 1.7, 1.5 and 4.7 on average of trachyte, trachyandesite, trachybasalt, basalt and pumice composition respectively. Trachyte is higher in SiO_2 and K_2O (64.5% & 4.6% respectively) and lower in Al_2O_3, TiO_2, Fe_2O_3, CaO and P_2O_5 (13.41%, 0.4%, 6%, 1.8% &0.3% respectively) than other volcanic rocks. Al_2O_3 and MnO contents are high in trachybasalt (17% and 0.4%, respectively). Basalt samples have the highest content of CaO, MgO and P_2O_5 (8.8%, 7.5 % and 0.7%, respectively), and have the lowest Na_2O content (3.1%). TiO_2, Fe_2O_3 and Na_2O content (3.2%, 14% and11%, respectively) are the highest and SiO_2 and K_2O (31.6% &1% respectively) are the lowest in pumice.

4- The general geochemical features from the trace data are as follows: Ba is high in the trachytic volcanic rocks (Av. =1158 ppm) while basaltic volcanic rocks have the highest Sr, Cr and Ni (Av.=725, 229&134 ppm, respectively). The highest HFSE (Hf=17.7 ppm and Ta=8.5 ppm) are recorded in trachyte volcanic rocks. The high cotents of Zr and Y in the studied volcanic rocks is a feature of within plate felsic igneous rocks (Bowden and Turner., 1974).

5- Rb/Sr ratio is a good manifestation of a typical magmatic differentiation trend. Among the studied volcanic rocks, there is a progressive increase in the Rb/Sr ratio with increasing differentiation as observed in Table (3) from trachytic volcanic rocks (Av.=0.4), trachyandesite (Av.=0.5) and trachybasalt (Av.=0.2). The average ratios of Ba/Sr (5 for trachyte, 4.6 for trachyandesite, 4 for trachybasalt and 1.5 for pumice volcanic rocks) are considerably higher than the characteristic averages for calc-alkaline andesites (Ba/Sr=0.7) given by Taylor (1969).

Geochemical Classification

The total alkalis-SiO_2 variations diagram is recommended by the IUGS Subcommittee for the classification of volcanics rocks (Le Maitre, 1989; Le Bas and Streckeisen, 1991). The Plotting of the studied volcanics in such diagram (Fig.18) indicates clearly that the analyzed samples lie in trachyte, trachyandes-

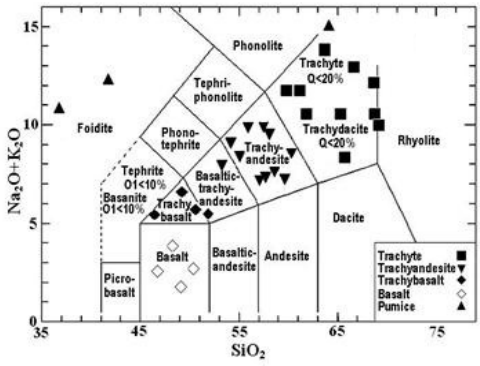

Fig.18: Total alkalis (wt %) versus silica content (wt %) (TAS) diagram for the studied volcanic rocks of Le Maitre (1989)

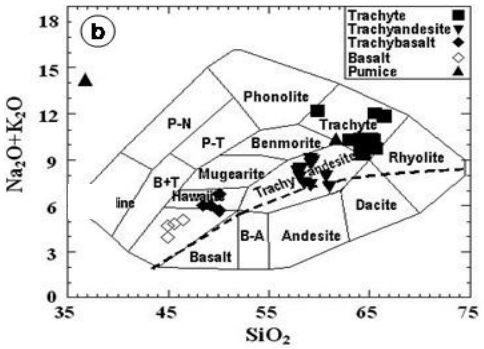

Fig.19: Total alkalis (wt %) versus silica content (wt %) of Cox et al., (1979). Dashed line represents the boundary line between alkalic and subalkalic rocks after McDonald

ite, trachybasalt and basalt fields. The binary diagram of total alkalis versus silica of Cox et al. (1979) (Fig.19) shows that the studied samples are clustered in the fields of trachyte, trachyandesite, hawaiite and basalt fields.

Magma Type

The K_2O (wt %) versus SiO_2 (wt %) binary diagram after Middlemost (1975) shows that the studied volcanic rocks are alkalic with general sodic trend as confirmed from the Na_2O/K_2O ratios. The clustering of the samples in two narrow SiO_2 range may suggest a degree of fractional crystallization (AFC) direction (Fig. 20)

On the other hand, Kuno (1966) and Irvine and Baragar (1971) used the TAS diagram to subdivide the volcanic rocks into two major magma series, alkaline and sub-alkaline. On the TAS diagram, the studied volcanic rocks plot in the alkaline field in two clusters reflecting a possibility of more than one magmatic pulse (Fig.21).

Tectonomagmatic Environments and Petrogenesis

In order to decipher the paleo-tectonic settings of the volcanic rocks, several attempts were made using the behaviors and variation trends of their immobile major and/or trace elements. The triangular diagram of Pearce et al. (1977), involving the investigated rocks

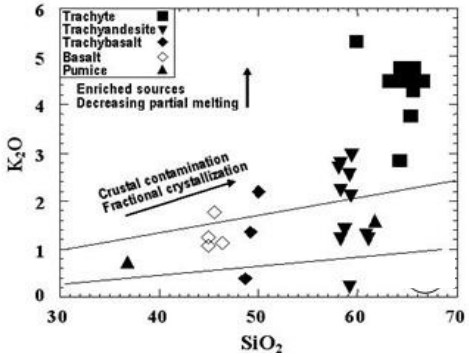

Fig.20: K_2O (wt %) versus SiO_2 (wt %) for the studied volcanic rocks .Field boundaries after Middlemost (1975)

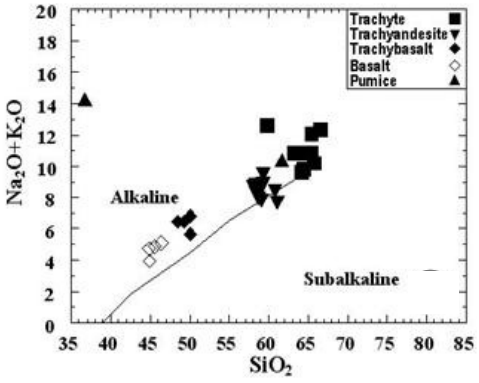

Fig.21: Total alkalis (wt %) versus silica content (wt %) of Irvine and Baragar (1971)

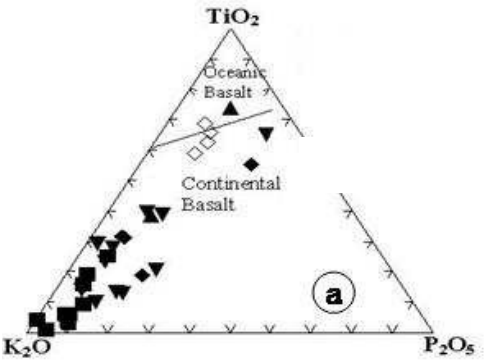

Fig.22: TiO_2-K_2O-P_2O_5 ternary diagram for tectonic setting discrimination of the studied volcanics, after pearce et al., (1977)

shows that the studied volcanics plot in the continental basalt field (Fig.22).

The (Al_2O_3/TiO_2)-TiO_2(wt %) binary diagram of Sun and Nesbit, (1978) and Sun (1980) shows that the studied volcanic rocks are plotted in a linear or slightly curved pattern (Figs. 23&24). This pattern suggests that they might be a result of a continuous magmatism and that they were derived from the same magma source by fractionation processes. The high TiO_2 magma is being the early fractionated, while the low TiO_2 magma is produced from the more fractionated varieties. The fractionation of olivine and plagioclase can not explain the observed trends. CaO/Al$_2$O$_3$ vs. SiO$_2$ variation diagrams (Fig.24) but

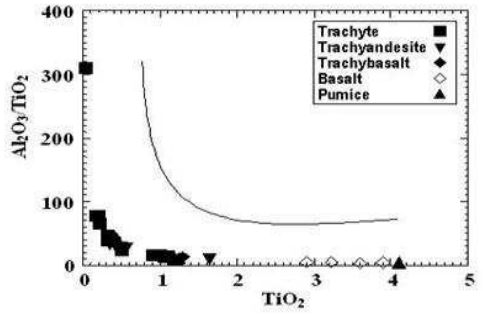

Fig.23: Binary diagram of Al_2O_3/TiO_2 vs. TiO_2 plot after Sun and Nesbit, (1978) showing petrogenetic aspects of the investigated rocks

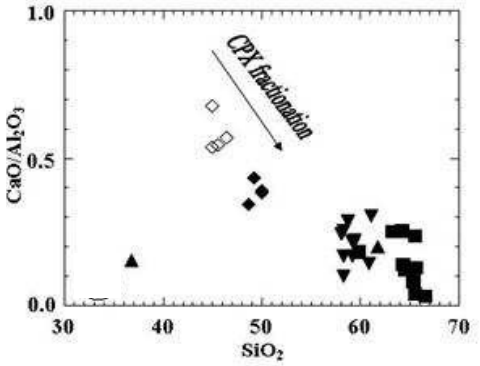

Fig.24:Binary diagram of CaO/Al_2O_3vs. Sio_2 showing petrogenetic aspects of the investigated rocks

the fractionation of these phases together with $CaO > Al_2O_3$ is required. Clinopyroxene is a good candidate. Titanaugite is present in the phenocrystal assemblage as well as an abundant phase in the groundmass.

On the AFM diagram (Fig.25) of Irvine and Baragar, (1971) superimposed by tectonic trends by Petro et al., (1979), The studied volcanic samples are plotted close to the total iron apex (A-F) parallel to the extensional intra-plate rift-related trend. The samples are plotted on the tholeiitic affinity. Therefore, it is suggested that the studied volcanic rocks

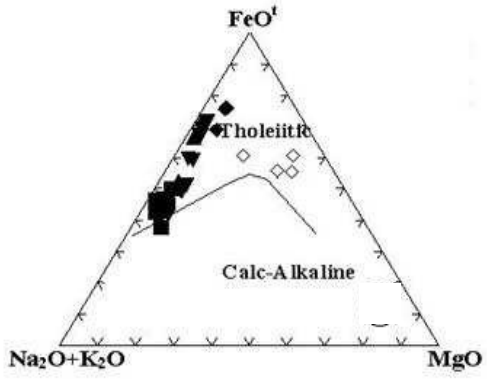

Fig.25: $Na_2O + K_2O$- FeO^t- Mgo ternary diagram of the chemical characters and magma type of the investigated rocks, after Irvine and Baragar, (1971)

originated from a tholeiitic magma rich in total iron and total alkalis content.

Distribution of Rb and Sr is controlled mainly by the abundance of potash feldspars (essentially for Rb and to a less extent for Sr), and the abundance of Ca-plagioclase (for Sr). Both K-feldspar and Ca-plagioclase are directly related to crustal fractionation and hence to its thickness. Plotting the relationship between incompatible elements Rb-Ba, Sr-Rb and Ba-Sr for the studied volcanic rocks shows normal fractional crystallization trends that are consistent with the predominance of alkali feldspar and clinopyroxene as fractionated phases (Figs.26a-d). On the Ba/Zr versus Rb (ppm) binary diagram (Fig.26d), the AB trend represents fractional removal of the mineral assemblage's olivine, clinopyroxene, plagioclase and magnetite from a basaltic source. The BC trend reflects extraction of the remaining melt at stage B followed by fractionation of clinopyroxene, plagioclase, K-feldspar and magnetite. The studied volcanic rocks imply a significant degree of fractional crystallization along trend BC.

This leads to the conclusion that the trachytic magma did not incorporate significant amount of crust that in turn does not affect the gross ultimate composition of the trachyte.

Rare Earth Elements (REEs)

REEs tend to concentrate in residual magma and occur in accessory minerals such as zircon, allanite, apatite, monazite, xenotime, fluorite and sphene as well as significant amounts of REE could occur in feldspars, pyroxenes and amphiboles.

Generally, the light REE (LREE) tend to be concentrated in monazite and apatite, while heavy REE (HREE) tend to be concentrated in garnet, xenotime , fluorite and zircon. Rare Earth elements of even atomic numbers are more stable and more abundant than the adjacent odd atomic number ones. This difference as well as the small and steady decrease in ionic size with increases atomic number (i.e, lanthanide contraction) leads to the fact that the rare earth elements become fractionated relative to each other.

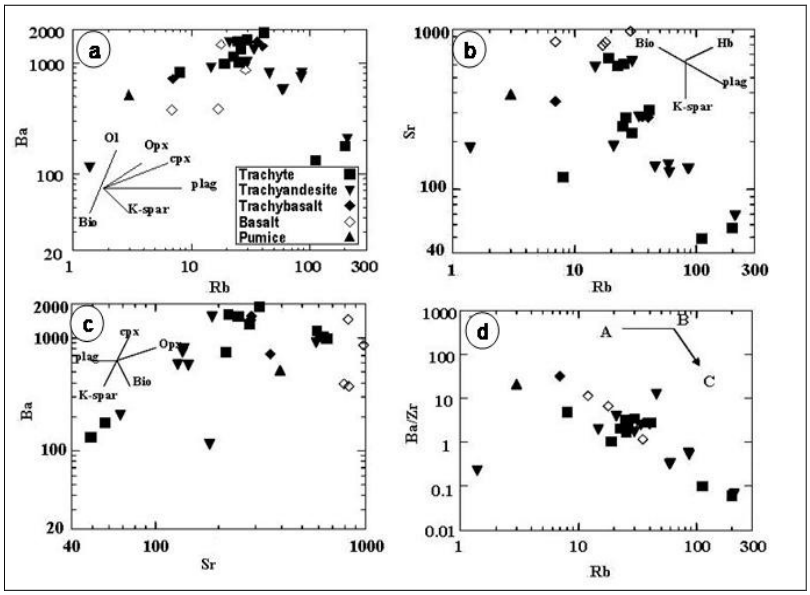

Fig. 26: Binary diagram between selected trace elements, the mineral vector diagram illustrating a fractional crystallization model (After Arth, 1976)

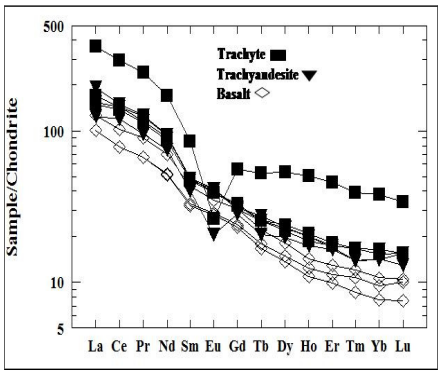

Fig.27: X-ray diffractogram and EDX spectrum of kasolite, which recorded at G. El Ghurfa, Gaziret Khashm Natash and Western Ghurfa, south Eastern Desert.

The normalized REEs patterns (Fig.27) shows the extreme depletion of the HREEs (21.8-44ppm) relative to the LREEs (182-391ppm) which is most likely due to the presences of monazite and xenotime in the source.

Zircon has an effect similar to that of monazite and xenotime deplete in the heavy REEs. Monazite and allanite cause some enrichment in the light REE. The general increase in the REE contents accompanied by pronounced deepening of the negative Eu anomaly in these volcanic may suggest that they were evolved by fractional crystallization.

Europium (Eu) anomalies,($Eu/Eu^* = Eu_N / \sqrt{Sm_N . Gd_N}$) are mainly controlled by plagioclase fractionation especially in felsic magmas. Thus, removal of feldspars from a felsic melt by crystal fractionation or by partial melting of a rock in which feldspars are retained in the source will give rise to negative Eu anomaly in REE patterns. The -ve Eu anomaly could be due to low-pressure fractionation of plagioclase that led to depletion in Sr and Eu.

The perceptible negative Eu anomaly is either due to the partitioning of Eu into feldspar during fractionation, which is an important process in developing peralkalinity, or the presence of residual feldspar in the source (Singh et al., 2006). Another alternative explanation for the negative Eu anomaly is based on the high oxygen fugacity in the melt due to volatile saturation (Grenne and Roberts., 1998).

CONCLUSIONS

Two ring structures (Gaziret Khashm Natash and Western Ghurfa) and one ring dyke (G. El Ghurfa) have extruded through the three volcanic flows, particularly in the eastern area. The three rings range in composition from volcanic flows (represented by trachybasalt, trachyandesite, normal and alkaline trachyte) to volcaniclastic sediments (tuffs and agglomerates).

According to the results revealed from the mineralogical studies, the study volcanic rocks contain meta-autunite and kasolite as uranium minerals, with association of molybdite, monazite, xenotime and allanite as accessories.

Geochemically, the investigated volcanic rocks are originated from an alkali magma rich in total alkalis, and similar to continental basalt. The studied rocks might be a result of a continuous magmatism and that they were derived from the same magma source by fractionation processes.

The high TiO_2 magma is being the early fractionated, while the low TiO_2 magma is produced from the more fractionated varieties. The studied volcanic rocks imply a significant degree of fractional crystallization along trend BC. This leads to the conclusion that the trachytic magma did not incorporate significant amount of crust that in turn does not affect the gross ultimate composition of the trachyte.

The observed enrichment in the REE of the studied volcanic rocks is mainly due to increasing their LREE abundances. The studied volcanic rocks have steep LREE, nearly flat HREE and a negative Eu anomaly. The –ve Eu anomaly is either due to the partitioning of

Eu into feldspar during fractionation, which is an important process in developing alkalinity, or the presence of residual feldspar in the source (Singh et al., 2006). Another alternative explanation for the negative Eu anomaly is based on the high oxygen fugacity in the melt due to volatile saturation (Grenne and Roberts, 1998). The low Y and REE contents result from sub-solidus metasomatic effects which led to the mobilization of these elements in the form of carbonate complexes.

Uranium which measured chemically more than equivalent uranium in the study samples. The U-bearing solutions have been originated by leaching from normal trachyte or by ascending hydrothermal solutions (oxidizing environments) along channel ways faults. The secondary uranium minerals formed by the combination of the U-bearing solutions with other cations such as Ca, Pb, and anions such as P_2O_5 and SiO_2 (forming meta-autunite and kasolite).

REFERENCES

Abul Gadayel, A. A., 1974. Contribution to geology and geochemistry of Wadi Natash lava flows. M. Sc. Thesis, Fac. Sci., Cairo Univ., Cairo, 212p.

Arth, J. G.,1976. Behavior of trace elements during magmatic processes. A summary of theoretical models and their applications. J. Res. U.S. Geol. Surv.,4, 41-47.

Barthaux, J. C.,1922. Chronologie et description des roches ignées du Desért Arabique. Mem. Inst. D'Egypt. Le Cairo, Tom 5.

Bowden, P., and Turner, D. C.,1974. Peralkaline and associated ring complexes in the Nigeria-Niger Province, West Africa. In: The alkaline rocks(Sorenson, h., ed.): John Wiley and Sons Ltd., London, 330-351.

Coulter, D.H.,1981. Petrology and stratigraphy of the Wadi Natash Volcanics, Eastern Desert, Egypt . M.A.Thesis, Bryn Mawr College, Bryn Mawr, U.s.A.

Cox, K. G.; Bell, J. D., and Pankhurst, R. J.,1979. The interpretation of igneous rocks. George Allen & Unwin, London, 450p.

Crawford, W. A.; Coulter, D. H., and Hubbard, J. H. B.,1984. The aerial distribution, stratigraphy and major element chemistry of the Wadi Natash Volcanic series, Eastern Desert, Egypt. J. Afr. Earth Sci., 2, 119-128.

El Ramly, M. F.; Budanov, V.I., and Hussein, A. A.A.,1971. The alkaline rocks of south eastern Egypt. Geol, Surv. Egypt, Pap.53,111.

Grenne, T., and Roberts, D.,1998. The Holonda porphyrite, Norwegian Caledonides; geochemistry and tectonic setting of Early-Mid. Ordovician shoshonite volcanism. J. Geol. Soc., London, 155, 131-142.

Hansink, J. D.,1976. Equilibrium analyses of sandstone rollfront uranium deposits. Inter. Atomic Energy Agency, Vienna, 683-693.

Hashad, A.H., and El Reedy, M.W.M.,1979. Geochronology of the anorogenic alkalic rocks, South Eastern Desert, Egypt. Ann. Geol. surv. Egypt, 9, 81-101.

Hashad, A.H.; Hassan, M.A., and Aboul Gadayel, A.A, 1982. Geological and petrological study of Wadi Natash late Cretaceous volcanics, Egypt. J. Geol., 26, 19-37.

Hubbard, HB.,1981.Geochemical evolution of the Wadi Natash volcanics field and alkaline basalt flood in the Eastern Desert of Egypt. M.Sc. Thesis, Univ. South Carolina. U.S.A.

Ibrahim, M. E.,2010. Laterites Bearing- REEs, Wadi Natash, Southeastern Desert, Egypt. J. Rare Earth, 28, No.3, 471-476.

Ibrahim, M.E.; Aly, G.M., and El-Tohamy,

A.M.,2013. Mineralogical and Geochemical Aspects of Nubia Sandstones at Gabel El Ghurfa, Southeastern Desert, Egypt. Arab J. N. Sci. Appl., 45(2), 117-129 .

Irvine, T. N., and Baragar, W. R. A.,1971. A guide to the chemical classification of the common volcanic rocks. Canad. J. Earth Sci.,8,523-548.

Keer, P. F.,1977. Optical mineralogy. 4th Ed., McGraw-Hill Book Co., London, 617p.

Kuno, H.,1966. Lateral variation of basalt magma type across continental margin and island arcs. Bull. Volcanol., 29, 195-222.

Le Bas, M. I., and Streckeisen, A. L.,1991. The IUGS Systematic of igneous rocks. J. Geol. Sci. London, 148, 825-833.

Le Maitre, R.W.,1989. A classification of igneous rocks and glossary terms; Recommendations of the international Union of Geological Sciences subcommission on the systematic of igneous rocks. Blackwell Scientific Publ., Oxford, 193p.

Middlemost, E. A. K.,1975. The basalt clan. Earth Sci. Rev., 11, 337-364.

Mohamed, F.H.,2001.The Natash alkaline volcanic field, Egypt; geological and mineralogical inference on the evolution of basalt to rhyolite eruptive suit. J. Volcan & Geotherm. Res., 105, 291 – 322.

Pearce, J. A., and Gale, G. H.,1977. Identification of ore deposition environment from trace element geochemistry. Dprc. Publ. Geol. Lond., 7, 14-24.

Petro, W. L., Vogel, T. A., and Wilband, J. T.,1979. Major element chemistry of plutonic rock suites from compressional and extensional plate boundaries. Chem. Geol., 26, 217-235.

Ressetar, R.; Nairn, A.E.M., and Monrad, J.R.,1981. Two phases of Cretaceous- Tertiary magmatism in the Eastern Desert of Egypt; paleomagnetic, chemical and K-Ar evidence. Tectonophysics,73,169-193.

Shapiro,L., and Brannock, W.W.,1962.Rapid analysis of silicate , carbonate and phosphate rocks, U.S. Geol. Surv. Bull,114 A,56p.

Singh, A. K.; Singh, R. K. B., and Vallinayagan, G.,2006. Anorogenic acid volcanic rocks in the Kundal area of the Malani igneous suite, Northwestern India; geochemical and petrogenetic studies. J. Asian Earth Sci., 1-14.

Stuckless, J. S.; Nkomo, I. T.; Wenner, D. B., and Van Trump, G.,1984. Geochemistry and uranium favourability of the postorogenic granites of the northwestern Arabian Shield. Kingdom of Saudi Arabia. In: Pan-African crustal evolution in the Arabian-Nubian Shield (Convenor, A., Al Shanti,M.,Ed.): Bull. Fac. Earth Sci., king Abdelaziz Univ., Jeddah, Pergamon Press, Oxford,195-210.

Sun, S. S., and Nesbit, R. W.,1978. Petrogenesis of Archean ultrabasic and basic volcanics; evidence from rare earth elements. Contrib. Mineral. Petrol., 65,301-325.

Sun, S.S.,1980. Lead isotopic study of young volcanic rocks from mid-ocean ridges, ocean islands and island arcs. Philosophical Transactions of the Royal Society of London, Series A ,297,409–445.

Taylor, S. R.,1969. Trace element chemistry of andesites and associated calc-alkaline rocks. In: Proceedings of the Andesite Conference (McBirney, A. P.,Ed.): Oregon Dept. Geol. and Mineral Ind.

الخصائــص الجيوكيميائية والمعدنيــة لبركانيــات نتش، جنـوب الصحــراء الشرقيــة مصـــــــــــــر

مصطفى السيد محمد درويش وأميرة محمد التهامى

إن تراكيب حلقتى غرب الغرفة وجزيرة خشم نتش بالإضافة الى القاطع الحلقى لجبل الغرفة قد تكونت من خلال تدفق الحمم البركانية اثناء النشاط البركانى ويتراوح تكوين هذه الحلقات الثلاث من الحمم البركانية المتمثلة بصخور البازلت والأنديزيت التراكيتى والبازلت التراكيتى مروراً بالتراكيت العادى والتراكيت القلوى إلى الصخور الفتاتية المتهشمة مثال الاجلوميريت وفتات بيوميس وسكوريا، وتتخذ هذه الحلقات الشكل الدائرى أو النصف دائرى وتتراوح فى القطر من ٠,٦كم الى ١كم . إن المحتوى العالى من اليورانيوم فى هذه الصخور محل الدراسة إنما يرجع الى وجود معادن يورانيوم ثانوية مثل الميتاأتونيت والكازوليت بالإضافة الى المعادن المكملة الحاملة لليورانيوم مثل المونازيت، الزينوتيم، الزركون والألانيت. أثبتت الدراسات الجيوكيميائية للصخور البركانية أنها من نوعية صخور التراكيت، الأنديزيت التراكيتى، البازلت التراكيتى والبازلت وانها ذات أصل صهارة قلوية وتطورت فى بيئة بازلت قارية. إن الإثراء فى العناصر الأرضية النادرة الخفيفة التى تتراوح من ١٨٢ الى ٣٩١ جزء من المليون إنما يرجع الى وجود معادن المونازيت، الزينوتيم، الزركون والأ لنيت فى مصدر هذه الصخور.